Straight Line Segments Extraction and EKF-SLAM in Indoor Environment

Jixin Lv[1], Yukinori Kobayashi[2], Ankit A. Ravankar[1], and Takanori Emaru[2]
[1]Graduate school of Engineering, Hokkaido University,Sapporo, Japan
[2]Faculty of Engineering, Hokkaido Unicersity, Sapporo, Japan
Email: lvjixin@mech-hm.eng.hokudai.ac.jp; kobay@eng.hokudai.ac.jp; ankitravankar@gmail.com; emaru@eng.hokudai.ac.jp

***Abstract*—Thispaper presents a method of simultaneous localization and mapping (SLAM) in indoor environment using extended Kalman filter (EKF) with the straight line segments as the adopted geometrical feature. By using conventional two dimensional laser range finder (LRF) as the main sensor, robot finds a number of points scanned from the surrounding environment.Split-and-Merge is one of the mostpopular algorithms to extract straight line segments from these raw scanned points. However, during the splitting procedure, especially when long range LRF is employed, the widely adoptedmethod named iterative end point fitting (IEPF) has difficulty to segment the points' cluster into collinear subsets correctly and sufficiently due to its constant splitting criterion.To solve this problem,we introduce modified iterative end point fitting (MIEPF) which calculates the splitting criterion for each cluster individually.Simulation and experimental results show the effectiveness of the proposed algorithm.**

***Index* Terms—line segment, modified iterative end point fitting, Split-and-Merge, EKF-SLAM**

I. Introduction

When a robot enters anunknown environment, in order to realize the autonomous navigation, the robot needs to acquire the model of the surroundings and estimate the own pose with respect to the environment. This problem is well known as simultaneous localization and mapping problem, which is commonly abbreviated as SLAM problem, has been investigated by many researchers[1]-[4]since it is a basic requirement for realizing effective autonomous robotic navigation and operation.

EKF-SLAMalgorithm, which utilizes the extended Kalman filter toSLAM using the maximum likelihood data association, might be the most influential SLAM algorithm.Typically, EKF-SLAM is feature based. For example, the points based EKF SLAM algorithm, whichhas been well investigated and detailed by researchers[5], [6]. However, comparing with the points based EKF-SLAM, straight line segments based EKF-SLAM is more intuitive and compactduring the real application in the indoor environment [7]. For this kind of EKF-SLAM application, the correct straight line segments extraction is one of the crucial problems.

Manuscript received September 1, 2013; revised November 27, 2013.

With regard to thesensor, two-dimensional laser range finder is one of the most popular sensors applied in SLAM for its high speed and good accuracy. And another merit is that it is robust to the variation of lighting and temperature conditions. Taking these advantages into consideration, we useLRF as robotic sensor.

The rest of this paper is structured as follows. Sections IIintroducesthe Split-and-Merge algorithm with MIEPF during the splitting procedure.Section III details the EKF-SLAM algorithm that employs line segments as the feature of the surrounding environment. The simulationand experiments in Section IVdemonstrate the effectiveness of the presented algorithm. Finally, Section V outlines several conclusions and future work.

II. Line Segments Extraction

A. Raw points and corresponding line

Before the line extraction, LRFis required to explore the environment in ashort time, thus acquires "n" scannedpointsp^i:

$$p^i = (x^i y^i)^{\mathrm{T}} = (r^i \cos\varphi^i r^i \sin\varphi^i)^{\mathrm{T}},\ \ i = 1,2,\dots n \quad (1)$$

where$r^i$is the distance between the i-th scanned point and the origin of LRF, φ^i is the angle of i-th scan point with respectto the X_r-axis of LRF's frame $O\text{-}X_rY_r$, as shown in Fig. 1.The task of the line extraction algorithm is to extract the parameters$\rho$and$\alpha$of the straight line segments from the raw points.

Nguyen et alconducted a comparison between the famous line extraction algorithms [8], based the conclusion of that comparison, we implement the Split-and-Mergealgorithm to extract the line segments in this research because of its superior speed and compatibility for the real-time SLAM application. The Split-and-Merge algorithm is mainly constructed by three procedures: split, straight line fitting and merge.

B. Split

Splitting procedure can be treated as a kind of data-preprocessing which splits the whole points into several collinear points' clusters. In our former research work [9], splitting procedure consists of adaptive breakpoint detector (ABD)[10][11]and iterative end point fitting (IEPF)[12].

doi: 10.12720/joace.2.3.270-276

ABD is apoint distance based segmentation method that separates the raw points into points'clusters.

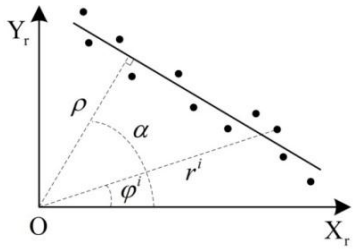

Figure 1. Geometry of scanned points and corresponding line.

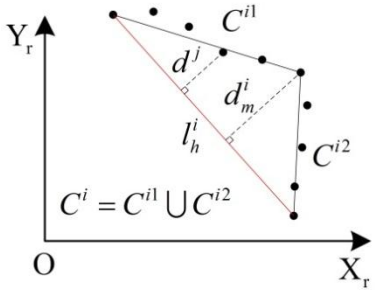

Figure 2. Principle of IEPF algorithm.

IEPF is a well-known recursive algorithm for line extraction. Fig. 2 demonstrates the principle of IEPF. For one cluster of pointsnamed C^i, this algorithm uses one hypotheticalline l_h^ithat links thetwoend points first.Then it calculatesdistancesof every point d^j to the line l_h^i so it canfindthe maximaldistance d_m^i .If $d_m^i > D_T$,IEPFsplits thecluster of points C^i into two subsets C^{i1} and C^{i2}, where D_T is the predefined splittingthreshold. This procedure is iterated to each subset until no new subsets can be found.

IEPF performs satisfactory when it is applied to deal with some raw data scanned by short range LRF since usually the LRF shows high accuracy when it scans some short-distance objects. The threshold D_T can be set to a small value and the points will be split sufficiently.

However, the performance of IEPF deteriorates when it is applied to the raw data scanned by long range LRF. The problem can be explained by using Fig. 3. There are two clusters of points, one is C^i which is scanned from a close object that is constructed by 2 line segments, while another one is C^j which is scanned from a far object that contains 1 line segment only. The dilemma happens that the classic IEPF cannot choose anappropriate threshold D_T which can split these two clusters properly. That is because the accuracy of the LRF decreases with the increase in the scanning range. Thus the noise in the C^j is bigger than the maximum distance d_m^i in the C^i.

To solve this problem, we introduceMIEPFwhich changes its splitting criterion from a constant value$D_T$to a variable depending on the parameter of the hypothetical line,$l_h = (\rho_h \alpha_h)^{\mathrm{T}}$.The principle of the MIEPF could be explained by using Fig. 4, for the measurement $p^i = (r^i \varphi^i)^{\mathrm{T}}$ whose reality is $p_r^i = (r_r^i \varphi_r^i)^{\mathrm{T}}$, because of the LRF's properties, the variance of r^i follows:

$$\sigma_{r^i}^2 = \sigma_{r_0}^2,\ r_r^i \le r_0 \tag{2}$$

$$\sigma_{r^i}^2 = (\varepsilon_0 r_r^i)^2,\ r_r^i > r_0 \tag{3}$$

where$\varepsilon_0$andr_0 are provided by the LRF manufacturer,$\sigma_{r_0}^2$ is the variance of the measurement at range r_0. Since r^i is the good estimation of r_r^i, the variance of r^i can be expressed as:

$$\sigma_{r^i}^2 = \sigma_{r_0}^2,\ r^i \le r_0 \tag{4}$$

$$\sigma_{r^i}^2 = (\varepsilon_0 r^i)^2,\ r^i > r_0 \tag{5}$$

d^i is the distance between p^i and l_h . From the geometrical relationship, d^i can be calculated as:

$$d^i = r^i \cos(\alpha_h - \varphi^i) - \rho_h \tag{6}$$

In order to define the splitting criterion properly, we hopeto find the relationship between the variance of d^i and the distance of the object.

Twosimple assumptionsare introduced here to simplify the deduction:

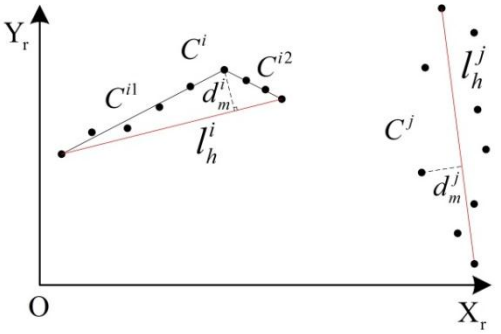

Figure3. Problem of the IEPF.

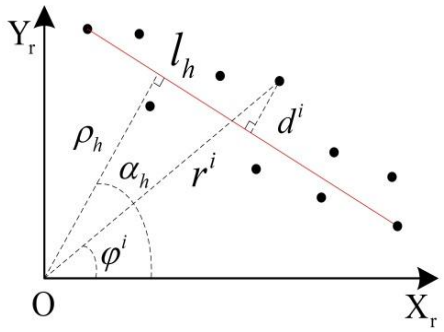

Figure4. Geometrical relationship between the noise and ρ_h.

1) Assume the noises of the LRF's measurements are Gaussiannoise and the variance of the φ^i, $\sigma_{\varphi^i}^2$ equals zero.
2) Assume the hypothetical line can well represent the object which contains 1 line segment only. Thus the covariance of its parameters can be neglected.

The first assumption has been widely adopted by researchers and the second assumption is also acceptable since this is a qualitative deduction.

Based on (6) and the assumptions, the variance of d^i can be obtained:

$$\sigma_{d^i}^2 = \left(\cos(\alpha_h - \varphi^i)\right)^2 \sigma_{r^i}^2. \tag{7}$$

By substituting (5) into (7), we can estimate the variance of d^i:

$$\sigma_{d^i}^2 \approx (\varepsilon_0 \rho_h)^2 \quad (8)$$

Based on this conclusion, we introduce the following equation to define the splitting criterion:

$$D_T = 3\sigma_{r_0} + \varepsilon(\rho_h - r_0) \quad (9)$$

where ε is one artificial setting ratio that takes the performance of the LRF and the user's experience into consideration. And the maximum D_{Tmax} will be set to restrict over loosing threshold based on the real performance of LRF.

C. Straight Line Fitting

We adopt the orthogonal least-squares method (OLSM) to fit the straight line segment from the collinear points' clusters fitting procedure. OLSM, which is also known as total least squares, fits the line by minimizing the sum of squared Euclidean distance between the points and fitted line.

Beyond the polar parameters of the line $l = (\rho \ \alpha)^{\mathrm{T}}$, OLSM also provides the covariance of the estimated parameters:

$$\Sigma_l = \begin{pmatrix} \sigma_\rho^2 & \sigma_{\rho\alpha} \\ \sigma_{\alpha\rho} & \sigma_\alpha^2 \end{pmatrix} \quad (10)$$

For more details about OLSM, please refer to [13].

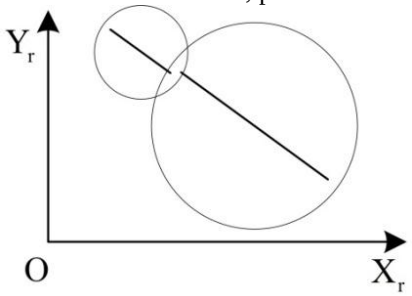

Figure 5. Line endpoints test.

D. Merge

In the mergeprocedure, the lines that close enough and have similar parameters will be merged into one line.We use "three steps identification"to find and check the similar lines.

First, we apply the coarse parameter test by setting thresholds T_ρ and T_α to find the line pairs thatare similar to each other.

Second, we execute the endpoints test to the candidate line pairs by setting two circles centered at the middle of the lines, as shown in Fig. 5. The diameter of the circle equals the length of the corresponding linewith asmall predefinedthreshold T_d. If one of the endpoints falls into another line's circle, then this line pair passes the endpoints test.

Finally, for the line pairl^i and l^j that satisfy the above criterions,we calculate theirMahalanobis Distance d_{ij} to distinguish whether they are qualified to be merged [14]:

$$d_{ij} = (\delta l)^T \left(\Sigma_{l^i} + \Sigma_{l^j}\right)^{-1} (\delta l) < \chi_l^2 \quad (11)$$

with

$$\delta l = l^i - l^j = \begin{pmatrix} \rho^i - \rho^j \\ \alpha^i - \alpha^j \end{pmatrix} \quad (12)$$

where $\chi_l^2 = 5.99$,for 95% confidence level.

If this condition holds, then the lines are sufficiently similar to be merged. We can derive the final merged line estimation using a maximum likelihood formulation and can calculate the final merged line coordinates l^{new} and uncertainty $\Sigma_{l^{new}}$ as follows:

$$\Sigma_{l^{new}} = \left(\left(\Sigma_{l^i}\right)^{-1} + \left(\Sigma_{l^j}\right)^{-1}\right)^{-1} \quad (13)$$

$$l^{new} = \Sigma_{l^{new}} \left(\left(\Sigma_{l^i}\right)^{-1} l^i + \left(\Sigma_{l^j}\right)^{-1} l^j\right) \quad (14)$$

III. Line Segments Based EKF-Slam

In EKF-SLAM, the map is represented as a large state vector stacking robot pose state$P$ and landmarksstate (or feature state)F,andit is modeled by a Gaussian variable [15]. This mapismaintained by the EKF through the processes of prediction (the robot moves) and correction (the robot observes the landmarks in the environment that had been previouslymapped).

At time *t*, the map state vector considering line segments as the features is expressed as:

$$\mu_t = (P^t \quad F^1 \quad \cdots \quad F^n)^{\mathrm{T}} \quad (15)$$

where"*n*" stands for "feature number".As shown in Fig. 6, the robot pose and the parameters of the feature with respect to the global frame O-$X_G Y_G$ are

$$P^t = \left(x_p^t \quad y_p^t \quad \theta_p^t\right), \quad F^n = (\rho_f^n \quad \alpha_f^n) \quad (16)$$

The covariance matrix of the state vector is

$$\Sigma = \begin{pmatrix} \Sigma_P & \Sigma_{PF^1} & \cdots & \Sigma_{PF^n} \\ \Sigma_{F^1P} & \Sigma_{F^1} & \cdots & \Sigma_{F^1F^n} \\ \vdots & \vdots & \ddots & \vdots \\ \Sigma_{F^nP} & \Sigma_{F^nF^1} & \cdots & \Sigma_{F^n} \end{pmatrix} \quad (17)$$

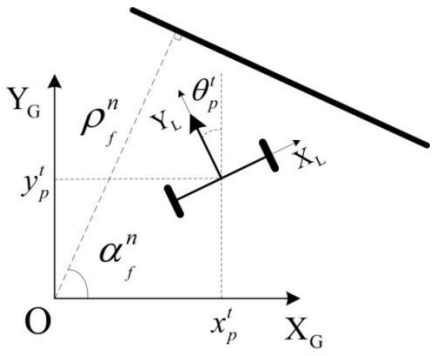

Figure 6. Geometrical relationship between the robot pose and feature parameters.

A. Robot Motion and EKF Prediction

Assume there are "*n*" features saved in state vector at time "*t*-1":

$$\mu_{t-1} = (x_p^{t-1} \quad y_p^{t-1} \quad \theta_p^{t-1} \rho_f^1 \quad \alpha_f^1 \ldots \rho_f^n \quad \alpha_f^n)^{\mathrm{T}} \quad (18)$$

When the robot is required to move a distance from time *t*-1 to time *t*, the measurement of the encoder from right wheel and left wheel within time "*t*-1" to time "*t*" is

$$u_t = (\Delta R \quad \Delta L) \quad (19)$$

The correspondingcovariance matrix of the measurement is

$$R_w = \begin{pmatrix} \sigma_{\Delta R}^2 & 0 \\ 0 & \sigma_{\Delta L}^2 \end{pmatrix} \quad (20)$$

The state vector and covariance matrix can be updated by

$$\bar{\mu}_t = g(\mu_{t-1}, u_t) \quad (21)$$

$$\bar{\Sigma}_t = G_p \Sigma_{t-1} G_p^T + G_w R_w G_w^T \quad (22)$$

with the Jacobian matrices $G_p = \frac{\partial g(\mu_{t-1}, u_t)}{\partial \mu_{t-1}}$ and $G_w = \frac{\partial g(\mu_{t-1}, u_t)}{\partial u_t}$.

After the movement, the LRF do the scan and find "*m*" observations (line segments):

$$z^i = (\rho_l^i \quad \alpha_l^i)^{\mathrm{T}}, i = 0,1 \ldots m \quad (23)$$

B. Observation and Feature Association

For all the observations, EKF-SLAM needs to execute the featureassociation which tries to associate the observations with the former features saved in the state vector so that EKF can correct the predicted state. In this part, we execute "three steps identification" again. After coarse parameter test and endpoints test which are described in the last section, the candidate association pair,observationz^i and featureF^jcan be find.The estimated observation of thefeatures $F^j = (\rho_f^j \quad \alpha_f^j)^{\mathrm{T}}$ should be

$$\hat{z}^j = h(\bar{\mu}_t) = \begin{pmatrix} \hat{\rho}_l^j \\ \hat{\alpha}_l^j \end{pmatrix} = \begin{pmatrix} \rho_f^j - \bar{x}_p^t \cos\alpha_f^j - \bar{y}_p^t \sin\alpha_f^j \\ \alpha_f^j - \bar{\theta}_p^t \end{pmatrix}. \quad (24)$$

The corresponding covariance matrixes of $\hat{z}^j$is

$$\hat{\Sigma}^j = H^j \bar{\Sigma}_t H^{j\mathrm{T}}, \quad (25)$$

with the Jacobian $H^j = \frac{\partial h(\bar{\mu}_t)}{\partial \bar{\mu}_t}$ and $\bar{\Sigma}_t$ is the covariance matrix of state vector that has been updated in the EKF predication procedure.For observed feature z^i and estimatedobservation $\hat{z}^j$, their Mahalanobis Distance is calculatedto distinguish whether they belong to the same feature:

$$d_{ij} = (z^i - \hat{z}^j)^{\mathrm{T}} \left(\Sigma^i + \hat{\Sigma}^j\right)^{-1} (z^i - \hat{z}^j) < \chi^2 \quad (26)$$

where$\chi^2$is the artificial criterion for this judgmentand Σ^i is the covariance matrix of the observation noise

$$\Sigma^i = \begin{pmatrix} \sigma_{\rho_l^i}^2 & \sigma_{\rho_l^i \alpha_l^i} \\ \sigma_{\alpha_l^i \rho_l^i} & \sigma_{\alpha_l^i}^2 \end{pmatrix} \quad (27)$$

If the judgment criterion (26) satisfied, then the observed feature z^i will be associated with features F^j.

C. EKF Correction

For the observation$z^i = (\rho_l^i \quad \alpha_l^i)^{\mathrm{T}}$ that are scanned at time *t*and has beenassociated with thefeature F^j, EKF-SLAM will implement thecorrection step to the state vector and its covariance matrix.

The EKF correction step is classically written as

$$K^j = \bar{\Sigma}_t H^{j\mathrm{T}} \left(H^j \bar{\Sigma}_t H^{j\mathrm{T}} + \Sigma^i\right)^{-1} \quad (28)$$

$$\mu_t = \bar{\mu}_t + K^j (z^i - \hat{z}^j) \quad (29)$$

$$\Sigma_t = (I - K^j H^j) \bar{\Sigma}_t \quad (30)$$

$K^j$is usually called Kalman gain, which is calculated by utilizing the uncertaintiesof the estimated observation and the real observation.After the Kalman gain has been calculated, the state vector and corresponding covariance are updated by(29) and (30).

D. New Feature Addition

For the observationz^i that failed to associatewith any detected features, EKF-SLAM will treat it as a new feature. Thus z^iwill become the $(n+1)^{th}$feature F^{n+1} in the state vector:

$$F^{n+1} = f(P^t, z^i) = \begin{pmatrix} \rho_f^{n+1} \\ \alpha_f^{n+1} \end{pmatrix} = \begin{pmatrix} \rho_l^i + x_p^t \cos\alpha_f^{n+1} + y_p^t \sin\alpha_f^{n+1} \\ \theta_p^t + \alpha_l^i \end{pmatrix} \quad (31)$$

And thecovariance matrix of the state vector also has to be augmented [16].

IV. Simulationand Experiments

A. Simulation of the MIEPF

Simulation is executed with the MIEPF setting $r_0 = 1000\text{mm}$, $\sigma_{r_0} = 15$ mm , $\varepsilon = 0.03$ and $D_{Tmax} = 220$ mm. The threshold of IEPF is $D_T = 220$ mm.

Fig.7(a) shows the simulated environment which is constructed by 6 objectswith increasing distances in clockwise direction. Each of the objects contains 2 long and parallel lines in the two sides and 1 orthogonal short linein the middle.

Fig. 7(b) shows the points scanned by the simulated LRF model. The LRF model is designed to scan objects with the distance from 0mm to 8000mm with the resolution 1mm and the angularscope is set from $-30°$ to $210°$ with the resolution $0.36°$. The Gaussian noise randomly generated by the programwas introduced to the measurement.

Fig. 7(c) andFig. 7(d) show the extracted lines based on the splitting results by applying IEPF and MIEPF, respectively. None of objects has been well split by IEPF while half of them are split by MIEPF correctly.

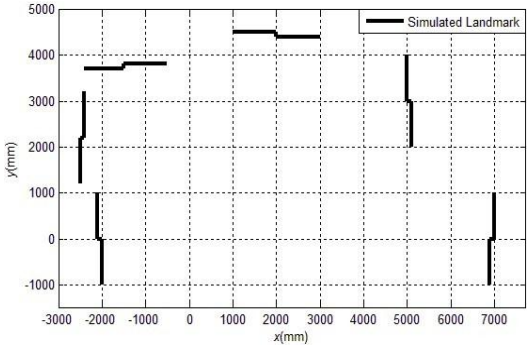

(a) Simulated landmarks.

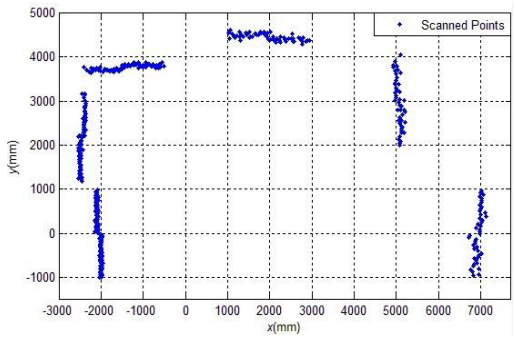

(b) Simulated scanned points.

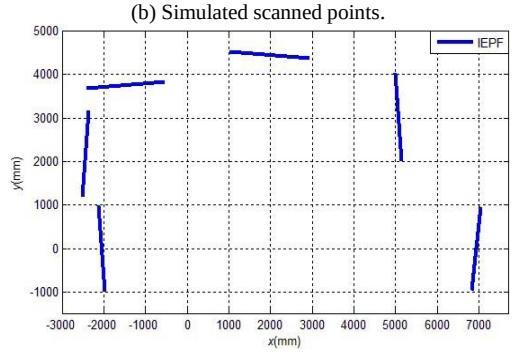

(c) Split by IEPF.

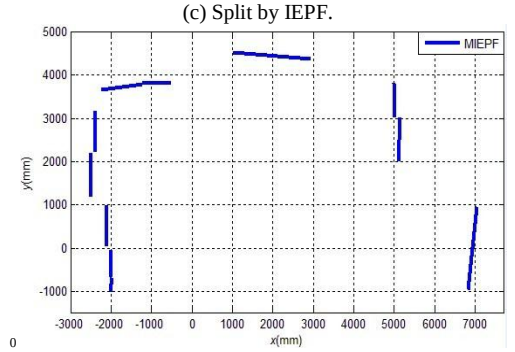

(d) Split by MIEPF.

Figure 7. Simulation of the comparison between IEPF and MIEPF.

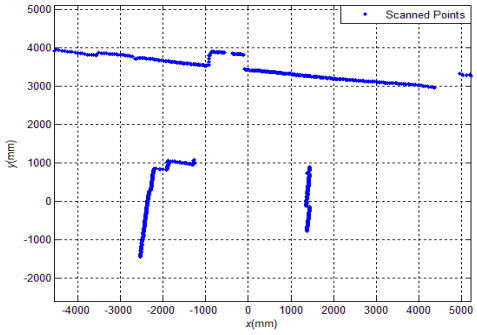

(a)Scanned points.

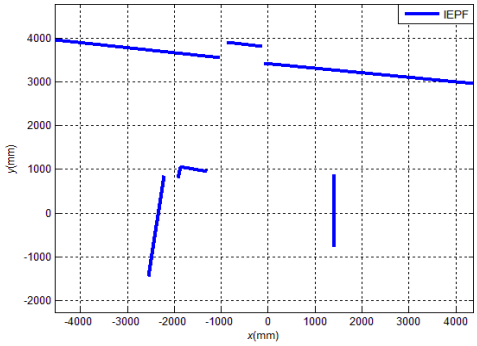

(b) Split by IEPF.

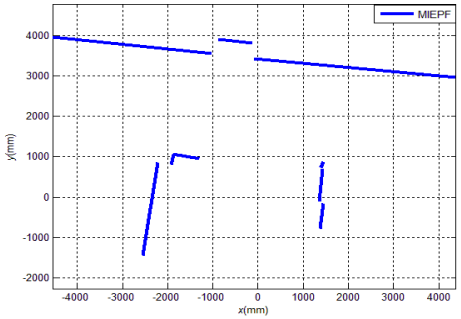

(c) Split by MIEPF.

Figure 8. Experiment of the comparison between IEPF and MIEPF.

B. *Experiment of the MIEPF*

In this experiment, the LRF UHG-08LX-Hokuyo whose scanning range covers from 100mm to 8000mm with the angular scope from $-30°$ to $210°$was applied to explore the environment.Fig.8(a) shows the raw points scanned by the LRF at one corner.

Line extraction is performed using the following MIEPF setting $r_0 = 1000$ mm , $\sigma_{r_0} = 10$ mm , $\varepsilon = 0.02$ and $D_{Tmax} = 150$ mm . The threshold of IEPF is $D_T = 150$ mm.

Fig. 8(b) and Fig. 8(c)show the extracted lines based on the splitting resultsby using IEPF and MIEPF, respectively. Notice that the lower right object is not split properly by IEPF while it is successfully segmented by MIEPF.

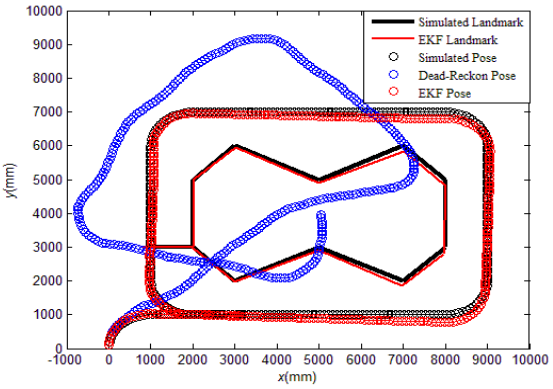

Figure 9. Simulation of the EKF-SLAM.

C. *Simulation of the EKF-SLAM*

Fig. 9 shows the final localization and mapping result of the straight line segments based EKF-SLAM. The black line segments are the simulated landmark while the red line segments are the mapping result finished by EKF-SLAM. The black small circlesare the simulated robot pose at each step. The red small circles stand for the robot pose estimated by EKF while the blue small circlesarethe robot pose estimated by the dead-reckoning method. This simulation result verifies the validity of the EKF-SLAM.

D. *Experiment of the EKF-SLAM*

During the experiment, the robotturns leftfirst, and then move along along and straight corridor.

Fig. 10 shows the localization (green curve) and mapping (red lines) result based on the dead-reckoning

localization method.This map is simply constructed by adding every scanned line without any merging. Although the performance of the encoder is much better than what we simulated, the error of the reckoning route is unbounded as the error accumulates with the robot movement.

Fig. 11 showsthe EKF-SLAM result. The EKF algorithm significantly corrects the localization result and the lines are merged well. Although the mapped corridor is not strictly straight for having someslight left shift, the mapping result is acceptable since the left shift brought by the dead-reckoning has been well corrected.

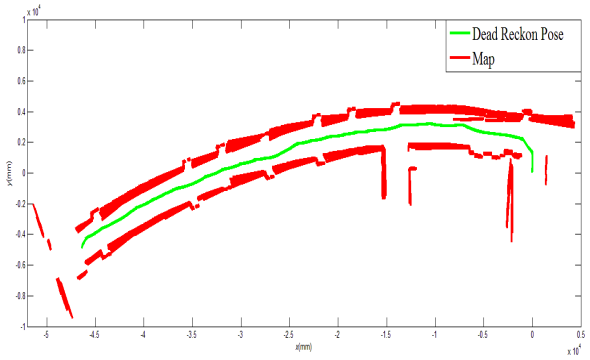

Figure10. Localizationand mapping result based on the dead-reckoning localization method.

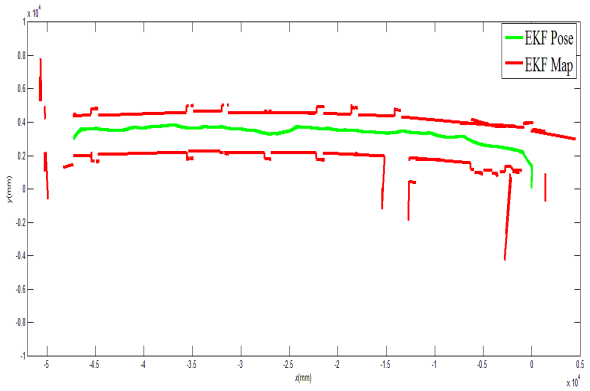

Figure11. Localizationand mapping result based on the EKF-SLAM method.

V. Conclusion and Future Work

The research work in this paper first introduced MIEPF into the famous Split-and-Merge line extraction. Comparing with the traditional IEPF method, the MIEPF shows the superior performance during the points splitting procedure after introducing the floating splitting criterion. After that, the EKF-SLAM algorithm which adopts the line segment as the feature has been detailed. Althoughthe feature associationbecomes more complicated by using line segment in comparison with the points since line segments have to take the endpoints into consideration, the proposed three step identification is straightforward and rigorous. For each part,the simulation and experimental results have been presentedto verify the effectiveness of the algorithms.

Our immediate next work would be continuing the SLAM research work to realize the loop closure and autonomous navigation. After that, we will introduce 3D SLAM work for the robot navigation in the indoor environment by multi-sensor fusion. And our final goal is to enable robot to navigate autonomously in unstructured indoor and outdoor environment.

Acknowledgements

This research is supported by the China Scholarship Council under grant number 2011632061and Hokkaido University.

References

[1] S. Se, D. G. Lowe, and J. J. Little, "Vision-based global localization and mapping for mobile robots," *IEEE Trans. Robot*., vol. 21, no. 3, pp. 364–375, 2005.

[2] A. Reina and J. Gonzalez, "A two-stage mobile robot localization method by overlapping segment-based maps," *Robotics and Autonomous Systems*, vol. 31, pp. 213-225, 2000.

[3] S.Y. An, J. G. Kang, L. K. Lee, and S. Y. Oh, "Line segment-based indoor mapping with salient line feature extraction," *Advanced Robotics*, vol. 26, pp. 437-460, 2012.

[4] J. E. Guivant and E. M. Nebot, "Optimization of the simultaneous localization and map-building algorithm for real-time implementation," *IEEE Trans. Robot. Autom.*, vol. 17, no. 3, pp. 242–257, May 2001.

[5] L. M. Paz, J. D. Tardos, and J. Neira, "Divide and conquer: EKF SLAM in O(n)," *IEEE Trans. Robot.*, vol. 24, no. 5, Oct 2008.

[6] T. Bailey, J. Nieto, J. Guivant, M. Stevens, and E. Nebot, "Consistency of the EKF-SLAM algorithm," in *Proc. IEEE/RSJ Int. Conf. Intell. Robots Syst.*, 2006, pp. 3562–3568.

[7] Y. H. Choi, T. K. Lee, and S. Y. Oh, "A line feature based SLAM with low grade range sensors using geometric constraints and active exploration for mobile robot," *Autonomous Robots*, vol. 24, no. 13–27, pp. 13–27, 2008.

[8] V. Nguyen, A. Martinelli, N. Tomatis, and R. Siegwart, "A comparison ofline extraction algorithms using 2D laser rangefinder for indoor mobilerobotics," in *Proc. IEEE/RSJ Int. Conf. IROS*, Edmonton, AB, Canada, 2005, pp. 1929–1934.

[9] J. Lv, Y. Kobayashi, Y. Hoshino, and T. Emaru, "Slope detection based on orthogonal assumption," in *Proc. IEEE/SICE International Symposium on System Integration*, Fukuoka, 2012, pp. 61-66.

[10] C. Premebida and U. Nunes, "Segmentation and geometric primitives extraction from 2d laser range data for mobile robot applications," in *Robotica Scientific Meeting of the 5th National Robotics Festival*, Coimbra, Portugal, April 2005.

[11] G. A. Borges and M. J. Aldon, "Line extraction in 2D range images for mobile robotics," *Journal of Intelligent & Robotic Systems*, vol. 40, no. 3, pp. 267-297, 2004.

[12] R. O. Duda and P. E. Hart, *Pattern Classification and Scene Analysis. John Wiley & Sons*, USA: New York, Letter Symbols for Quantities, ANSI Standard Y10.5-1968, 1973.

[13] A. Garulli, A. Giannitrapani, A. Rossi, and A. Vicino, "Mobile robot SLAM for line-based environment representation," presented at the 44th IEEE Conference on Decision and Control, the European Control Conference, 2005.

[14] S. T. Pfister, S. I. Roumeliotis, and J. W. Burdick, "Weighted line fitting algorithms for mobile robot map building and efficient data representation," *IEEE International Conference on Robotics and Automation*, vol. 1, pp. 1304-1311, September 2003.

[15] J. Sol à, T. V. Calleja, J. Civera, and J. M. M. Montiel, "Impact of landmark parametrization on monocular EKF-SLAM with points and lines," *Int. Journal of Computer Vision*, vol. 97, no. 3, pp. 339-368, September 2012.

[16] J. Collier. (2009). SLAM Techniques and Algorithms. [Online]. Available:http://computerrobotvision.org/2009/tutorial_day/crv09 SLAMTutorial.pdf

Jixin LV received the B.E. degree in Mechatronics from Zhejiang University, Hangzhou, China, in 2011. He is currently working toward a Ph.D. degree in Graduate School of Engineering, Hokkaido University, Sapporo, Japan. His research interests include indoor SLAM, autonomous navigation and artificial intelligence.

Yukinori Kobayashi received B.E., M.E. and Ph.D. degree in Mechanical Engineering from Hokkaido University, Sapporo, Japan, in 1981, 1983 and 1986, respectively. He is currently a Professor at Hokkaido University, Sapporo. His research interests include vibration control of flexible structures, control problem of robots having flexibility, path planning and navigation of mobile robots, vibration analysis and nonlinear vibrations of continuous systems.

Ankit A. Ravankar received B.E. in Production Engineering from the University of Pune, Pune, India in 2009, and the M.E. Degree in Mechanical Engineering from Hokkaido University, Sapporo, Japan in 2012. Currently he is working towards his Ph.D. degree in the Graduate School of Engineering, Hokkaido University, Japan. He is a MEXT scholarship recipient from the government of Japan. His research interests include indoor SLAM, autonomous navigation, Computer Vision and Artificial Intelligence.

Takanori Emaru received the M.E. and Ph.D. degrees in electrical engineering from Hokkaido University, Japan, in 1998 and 2002, respectively. He was a Research Fellow of the Japan Society for the Promotion of Science at the University of Electro-Communications, Japan from 2004 to 2006. He was an Assistant Professor with Osaka Electro-Communication University from 2006 to 2007. Currently, he is an Associate Professor with Hokkaido University, Hokkaido, Japan. His research interests include the areas of robotics, navigation, sensor and nonlinear signal processing